Journal of ELECTRONIC MATERIALS, Vol. 45, No. 8, 2016
DOI: 10.1007/s11664-016-4559-5


# An Investigation of Ferrite and Nanocrystalline Core Materials for Medium-Frequency Power Transformers

SELAMI BALCI,[1,3] IBRAHIM SEFA,[2,4] and NECMI ALTIN[2,5]

1.—Graduate School of Natural and Applied Sciences, Gazi University, Ankara, Turkey. 2.—Faculty of Technology, Department of Electrical-Electronics Engineering, Gazi University, 06500 Besevler, Ankara, Turkey. 3.—e-mail: selamibalci@gazi.edu.tr. 4.—e-mail: isefa@gazi.edu.tr. 5.—e-mail: naltin@gazi.edu.tr

In this study, two transformers are designed using the ferrite N87 and the nanocrystalline core materials for the same power level and operating frequency. The operating frequency is defined as 10 kHz, which is suitable for both materials. Modeling and simulation studies have been performed with the same finite element analysis software and the obtained results have been reported. The nanocrystalline and the ferrite N87 core materials have been compared according to both electrical and mechanical parameters. In these comparisons, many features such as core and winding losses, flux distributions, leakage flux, efficiency, and both electrical and mechanical performance have been reported comparatively in the case of rectangular waveform excitation of the transformer. Obtained results show that the weight and the volume of the transformer are reduced and more compact transformer is designed by using the nanocrystalline core material. In addition, besides the core loss, winding losses are also reduced in this design.

**Key words:** Medium frequency, transformer design, core material, FEA

## INTRODUCTION

Transformers are commonly used for voltage matching purposes in many alternating current (AC) and direct current (DC) power systems. The basic design strategy followed in the transformer design process has been valid for a long time. However, transformers with smaller volume and lower loss can be produced with modern design concepts using recent innovations obtained in the performance of the core materials. On the other hand, while the transformers have been used only for line frequency (50/60 Hz) systems for 30 years, nowadays they are used in medium and high frequency systems by employing soft magnetic materials with the spread of the power electronic converters. Power electronic converter circuits such as DC/DC, DC/AC, AC/DC, and AC/AC are situated in modern systems such as the line interface of renewable energy sources, electric vehicles, uninterruptible power supplies and motor drive systems.[1–3] Transformers embedded in the power electronic circuits that are operated in the medium frequency (400 Hz–20 kHz) and high frequency (>>20 kHz) range have many important roles, such as providing galvanic isolation between the low voltage and the high voltage sides and voltage level conversion between the input and output. In addition, the leakage flux reactance of the primary side can be used as a series resonant component for soft-switching circuits.[4,5]

Losses and thermal behavior of the transformers are greatly affected by the waveform of the excitation voltage and the operating frequency.[6] The design method for the power distribution transformers operated with the line frequency and the sinusoidal excitation is called as “classical design method”.[7] However, in rectangular waveform or pulse width modulation (PWM) excited medium-/high-frequency applications, analysis of transformer losses and electromagnetic effects would require more complicated calculations.[8] The resultant harmonic components, which are related to the

(Received December 18, 2015; accepted April 19, 2016; published online May 10, 2016)

duty ratio and the operating frequency, enhance both the core and the winding losses, thereby leading to additional temperature rise in the case of those kinds of excitations.[9]

The silicon-doped steel alloy core materials (such as M4 and M5 type) satisfy the requirements for design of the line frequency transformer. However, such alloys are quite unsuitable for medium-/high-frequency transformers because of their thermal and electromagnetic specifications.[10] Thus, the soft magnetic materials (such as ferrite, amorphous, and nanocrystalline) have been developed for the medium-/high-frequency transformers used in power electronics circuits. Recently, 6.5% silicon-doped non-oriented SiFe alloys (Supercore) have been available for medium-frequency (MF) designs. Magnetic and electrical properties of these materials differ from each other. The core material type is determined by the designer according to the limiting values of the frequency-dependent saturation flux density and the specific core loss. Non-oriented 6.5% SiFe material is generally preferred in the lower band of the MF range (400 Hz–2 kHz) for the MF transformer design.[11] Although saturation flux density of the amorphous material is higher than nanocrystalline, emitted audible noise increases with operating frequency. In addition, in one of the earlier studies, the electromagnetic performance of the amorphous and nanocrystalline materials for the high-frequency transformers with toroidal core was compared, and the obtained results prove that the nanocrystalline material has better specifications in terms of losses and volume.[12] Furthermore, it is also reported that nanocrystalline materials perform better than the ferrite and amorphous materials in terms of losses for different excitation voltages in medium-/high-frequency applications.[13]

In addition, Steinmetz's equation is modified in order to analyze the core losses of the amorphous core transformers used in DC/AC inverters at 2 kHz. It is seen that, besides the operating frequency and the magnetic induction peak values, core losses also vary with the switching duty ratio under non-sinusoidal excitation.[14]

The metal oxides that are used in manufacturing of the ferrite materials have larger resistances when compared to the alloy core materials. Thus, less eddy current loss occurs for the high-frequency applications.[15,16] However, sizes of the ferrite materials limit the transformer design in high-power applications. There are no sizing limitations for nanocrystalline materials, and therefore, the transformer kW and MW range with power ratings can be designed with nanocrystalline core material. Thus, single-phase or three-phase transformers can be designed for the desired power value. Nanocrystalline ribbon material with relevant geometry of the core is obtained by wrapping the strip like the C-cores. In addition, core losses of the ferrite core transformer are higher than the nanocrystalline core transformer for the same operating frequency.[17] Thus, nanocrystalline materials have been used in medium-/high-frequency transformer design in recent years, especially for medium- and high-power applications.[18]

The magnetic polarization of the transformer versus the operation frequency curve of the nanocrystalline material is smoother. Therefore, use of the nanocrystalline core material removes the undesired harmonic voltage on the load side of DC-DC converter transformer. Actually, the transformer designed with the nanocrystalline core is accepted as a linear transformer.[19] The nanocrystalline material exhibits quite favorable performance according to a specific loss and magnetostriction value. However, specifications of the nanocrystalline material may change according to the manufacturer. The losses and the magnetic properties of the nanocrystalline materials manufactured by two different manufacturers are also tested and statistically analyzed. In addition, the two companies do not offer the same size product options in terms of geometrical dimensions.[20]

In this study, an MF transformer used in the single-phase full-bridge inverter circuit and excited with a 10-kHz rectangular waveform was designed. Two different core materials were used in the design stage, and then the performances of the MF transformers designed using ferrite N87 and Vitroperm 250F nanocrystalline core materials were tested and compared. Since the power level was the same for both designs, the dimensions of the transformer cores and resultant core losses were different. In this report, three-dimensional (3D) models of the cores and coils of the transformers are modeled with the Ansys-Maxwell software for finite element analysis (FEA) method. The power electronic circuit is modeled with Ansys-Simplorer software simulated together (co-simulation) in order to obtain more realistic operation conditions. Transformers with the nanocrystalline and ferrite core materials are compared in terms of mechanical design parameters, leakage inductance values, core and winding losses, and flux distributions on the cores. Obtained results show that losses, weight, and volume of the transformer with the nanocrystalline core is lower than the transformer with ferrite N87 core. Besides the compact structure and high efficiency, the availability of the nanocrystalline material for producing a high-power-capable core makes it advantageous for medium- and high-power transformers.

## COMPARISON OF THE CORE MATERIAL CHARACTERISTICS FOR MF TRANSFORMERS

Magnetic materials include manganese (Mn), zinc (Zn), iron (Fe), aluminum (Al), nickel (Ni), magnesium (Mg), cobalt (Co), silicon (Si), and the other metal oxides.[21] Therefore, the magnetic materials

are classified into three different categories such as soft ferrite materials, iron alloy materials, and powder (powder iron) materials. Although, the powdered iron materials have lower permeability, they have larger saturation flux values than the ferrite materials. Commercially available carbonyl iron, sendust (or KoolM$\mu$) and molypermalloy powder (MPP) core materials are useful for the inductors of the high-frequency converter circuits.[22] When saturation flux values, permeability values, specific core losses, and electrical characteristics are compared, it is seen that alloy materials and ferrite materials have different characteristics. The specific properties of the ferrite N87 and the nanocrystalline core materials that are used in this study as transformer core materials are given in Table I. It can be seen that the specific properties of the nanocrystalline core material used in this study are quite similar to the Vitroperm 250F and the Finement FT-3M nanocrystalline materials.[23–26]

## MF TRANSFORMER DESIGN

Design parameters of the MF transformer are determined for a given power value according to the specific properties of each core material and the operating frequency. The electrical and the magnetic design parameters that affect the sizing are given in Table II. These parameters represent the specifications of the designed transformer.

The flux value of the ferrite N87 material is equal to 2/3 of the nanocrystalline material at the 10 kHz operating frequency. Therefore, the cross-sectional area of the core for the ferrite material is greater than the cross-sectional area of the nanocrystal core. In the transformer design, the core cross-sectional area ($A_c$) and the window area ($W_a$) are the basis of the sizing strategy. Therefore, the area product ($A_p$) of the transformer can be expressed by Eq. 1 for a given power value ($VA$).[27]

$$A_p = A_c \cdot W_a = \frac{VA \cdot 10^4}{K_f K_{cu} B_{ac} f J} \quad (1)$$

The power handling capacity of the transformer is plotted as 3D graphics in Fig. 1 according to the operating frequency ($f$), the flux density ($B$), and the core size ($W_a$ and $A_c$). The flux density of the core material can be determined by this chart for a certain operating frequency, and thus the maximum power capacity can be estimated.

For example, a 40-kVA-rated output power can be provided for 0.3 T flux density by using nanocrystalline core material at the 10 kHz operating frequency. However, for the same core size, the power level can be increased up to 25 kVA for the ferrite N87 material, because its flux density is only 0.2 T. Therefore, transformer size will be different if the different core materials are used for the same power level and operating frequency values. The basic strategy in sizing is to get the highest power capacity value for the certain operating frequency, whereas choosing the core material can be finalized by the determination of the lowest core loss.

The cross-sectional area of the core and the window area are primarily determined from the area product value obtained from the core sizing. The nanocrystalline C-core is generated by using the ribbon width of 50 mm to obtain a 50 × 40 mm core cross-sectional area. Thus, the window height of the 100 × 0.4 mm foil can fit to the C-core dimensions that are shown in Table III and Fig. 2.

Dimensions of the ferrite N87 core have been determined for the same power capacity with the nanocrystalline C-core, as given in Table IV. As a result of lower permeability and saturation flux values of the ferrite material, the core cross-sectional area of the Ferrite core transformer is approximately 1.6 times larger than the transformer with the nanocrystalline core. In addition,

**Table I. Specific properties of the core materials[24–27]**

| Parameters | Material type | |
|---|---|---|
| | Ferrite N87 | Nanocrystalline |
| Base material | MnZn | $Fe_{73.5}Cu_1Nb_3Si_{15.5}B_7$ |
| Saturation magnetization (T) | 0.39 | 1.23 |
| Permeability ($\mu$) | 2200 | 5000–7000 |
| Curie temperature (°C) | 210 | 510 |
| Coercivity force, $H_c$ (A/m) | 21 | 0.8 |
| Mass density (kg/m$^3$) | 4850 | 7200 |
| Thickness (mm) | Block core | 0.033 |
| Electrical resistivity(Ω m) | 10 | $1.3 \times 10^{-6}$ |
| Conductivity (S/m) | 0.1 | 769,230 |
| Stacking factor | – | 0.78 |
| Specific core loss (W/kg) | | |
| 10 kHz (0.1 T) | 1.5 | 0.35 |
| 10 kHz (0.2 T) | 25 | 1.5 |
| 10 kHz (0.3 T) | 8.2 | 4 |

**Table II. Design parameters of the transformer**

| Design parameters | Value |
|---|---|
| Power | 35 kVA |
| Operating frequency ($f$) | 10 kHz |
| Current density ($J$) | 200 A/cm$^2$ |
| Flux density ($B_{ac}$) | (max. 0.3 T for nanocrystalline) (max. 0.2 T for N87 ferrite) |
| Window utilization factor ($K_{cu}$) | 0.2 |
| Wave form factor ($K_f$) | 4 |

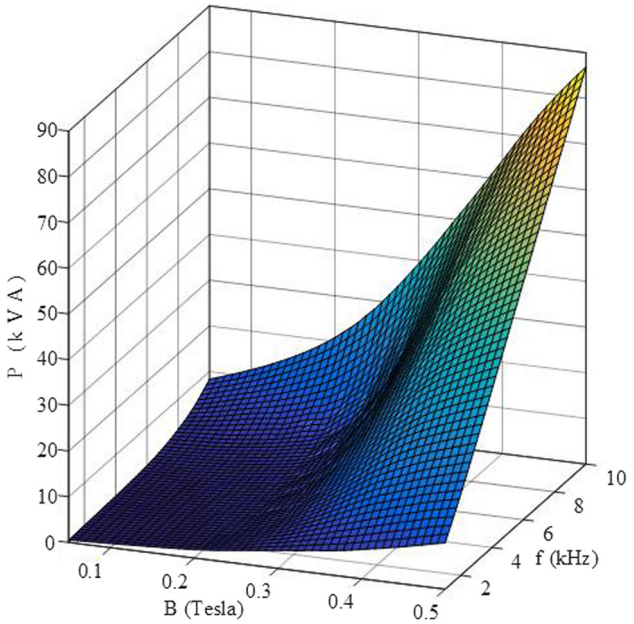


Fig. 1. Power handling capacity of the transformer.

the number of turns in each model is kept at the same value to provide a better comparison. The ferrite N87 (UU126/182/20) blocks are used for the ferrite core transformer as shown in Fig. 3.[26]

Winding region ($W_a$) changes according to the current density value ($J$), which determines the conductor cross-sectional area (see in Fig. 4). The window utilization factor ($K_{cu}$) is 0.2. Thus, the smallest winding volume is obtained with the nanocrystalline core material and 400 A/cm$^2$ current density at the forced air-cooled dry-type transformer.

## EXCITATION OF MF TRANSFORMERS WITH A RECTANGULAR WAVE VOLTAGE

In this study, two MF transformers with the different core materials were designed with the FEA method. In addition, the single-phase full-bridge inverter circuit given in Fig. 5 was designed with Ansys-Simplorer software to test the designed MF transformers.[4] Thus, both the power electronics and the electromagnetic models were simulated under the real operation conditions.

The MF transformers are usually excited with rectangular waveforms as shown in Fig. 6. According to this waveform, a voltage ($v_{(t)}$) given with Eq. 2 is induced by magnetic induction ($B_{(t)}$) depending on the number of turns ($N$) and the core cross-sectional area ($A_c$).[28]

$$v(t) = N\frac{d\varphi(t)}{dt} = NA_c\frac{dB(t)}{dt} \tag{2}$$

The flux density magnitude ($B_m$) for one period can be expressed as given in Eq. 3 because of the dead time ($T_0$). Thus, a number of turns can be obtained for the MF transformers as given Eq. 4[28]:

$$B_m = \frac{1}{2}\frac{V_{dc}}{NA_c}\left(\frac{T}{2} - T_0\right) \tag{3}$$

$$N = \frac{V_{dc}}{K_f f A_c B_m}\left(1 - \frac{T_0}{\pi}\right) \tag{4}$$

where the $V_{dc}$ is DC input voltage, $f$ is the operating frequency, $K_f$ is the form factor of rectangular waveform excitation voltage.

## MATHEMATICAL MODEL OF THE CORE LOSSES

Core losses ($P_{\text{core}}$) of the transformer are divided into two parts as the hysteresis loss ($P_h$) and the eddy current loss ($P_c$). In addition, the eddy current losses that are generated by voltage induced in the core laminations are divided into two parts, the conventional and the abnormal eddy current loss ($P_e$). Abnormal eddy current loss is effective under the non-sinusoidal excitation. The mathematical expression of the core losses is given in Eq. 5.[5,9,29]

$$P_{\text{core}} = P_h + P_c + P_e \tag{5}$$

This equation can be rewritten by substituting $P_h$, $P_c$ and $P_e$ equivalents, as given in Eq. 6:

$$P_{\text{core}} = K_h f B_{\max}^{x} + K_c (B_{\max} f)^2 + K_e (B_{\max} f)^{1.5} \tag{6}$$

where $K_h$ is the hysteresis coefficient, which is reduced with the increasing magnetic permeability. $B_{\max}$ is the peak value of flux density; $x$ is the Steinmetz coefficient varies between 1.5 and 2.5 according to the material permeability. Here, $f$ indicates the frequency of the excitation source in Hz. The eddy current coefficient is shown with $K_c$ and it varies depending on the thickness of the material, the packing factor and the electrical resistance values. Finally, $K_e$ is the abnormal eddy current coefficient.[7,29] In the single-phase full-bridge inverter circuit with the symmetrical rectangular waveform excitation, the magnetization period of the transformer varies with the operating frequency. Thus, the flux variation for a certain

**Table III. Sizing of the nanocrystalline C-core**

| *A* | *B* | *C* | *D* | *E* | *F* | $A_c$ | $W_a$ | $A_p$ | *MLT* |
|---|---|---|---|---|---|---|---|---|---|
| 40 mm | 45 mm | 120 mm | 50 mm | 125 mm | 200 mm | 20 $cm^2$ | 54 $cm^2$ | 1080 $cm^4$ | 28 cm |

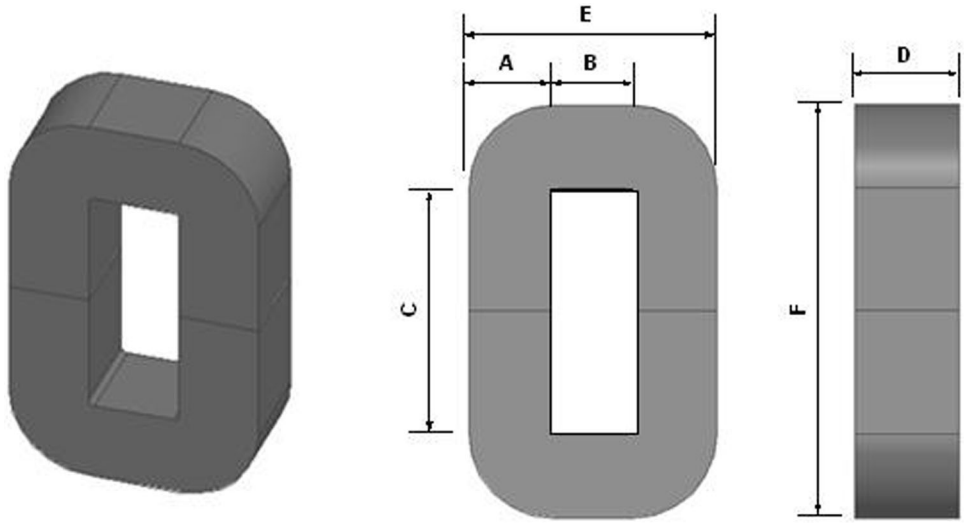


Fig. 2. Nanocrystalline C-core.

**Table IV. Sizing of the ferrite block core**

| *A* | *B* | *C* | *D* | *E* | *F* | $A_c$ | $W_a$ | $A_p$ | *MLT* |
|---|---|---|---|---|---|---|---|---|---|
| 28 mm | 70 mm | 126 mm | 120 mm | 126 mm | 182 mm | 33 $cm^2$ | 88.2 $cm^2$ | 2910 $cm^4$ | 40 cm |

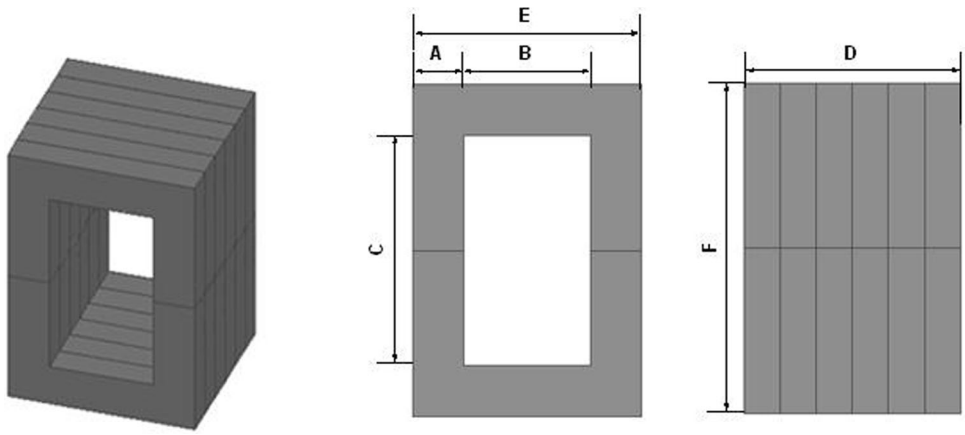


Fig. 3. Ferrite N87 block core.

operating frequency and a duty ratio ($D$) values can be written as in Eq. 7.[9]

$$\frac{dB(t)}{dt} = \frac{4B_{\max}f}{D} \tag{7}$$

Thereby, the core loss expression given in Eq. 6 can be extended for the rectangular waveform excitation as given in Eq. 8.[9]

$$P_{\text{core}} = K_h f B_{\max}^{x} + K_e \left(\frac{D}{4}\right)^{1.5} \left|\frac{dB}{dt}\right|^{1.5} + K_c \left(\frac{D}{4}\right)^{2} \left(\frac{dB}{dt}\right)^{2} \tag{8}$$

Here, $K_h$, $K_e$ and $K_c$ values are related to the core materials. Thus, the core loss of the transformer for the rectangular waveform excitation takes several values depending on the operating frequency, the flux density, the duty cycle and the core material type. The FEA software uses this mathematical model while calculating the core loss. The core loss coefficients of the nanocrystalline and the ferrite core materials operating at 10 kHz are given in Table V.

## EQUIVALENT CIRCUIT PARAMETERS OF THE TRANSFORMER

In order to obtain the equivalent circuit of the transformer, self and mutual inductance values of the primary and the secondary windings computed with the FEA software are used. Leakage inductance values of the designed transformers are related to the design geometry. Since the total volume of the transformer changes with the magnetic properties of the core material, the leakage flux values are also different for the ferrite and the nanocrystalline core transformers. However, the leakage inductance value ($L_{\text{leak}}$) is related to the mean length of the turns ($MLT$), as expressed in Eq. 9.[19]

$$L_{\text{leak}} = \frac{\mu_0}{I_1^2} \iiint H^2 dv \approx \frac{\mu_0 \cdot N_1^2 \cdot MLT \cdot B}{3 \cdot C} \tag{9}$$

The mean length of the secondary turns is greater than the primary turns. Thus, the leakage flux of the secondary is greater than the primary. In addition, the AC resistance values of the primary and the secondary windings can be determined by Eq. 10 according to the Dowell equation.[27,28,30]

$$\text{RF} = \frac{R_{ac}}{R_{dc}} = \Delta' \left[\xi_1 + \eta_w^2 \frac{2}{3}\left(m^2 - 1\right)\xi_2\right] \tag{10}$$

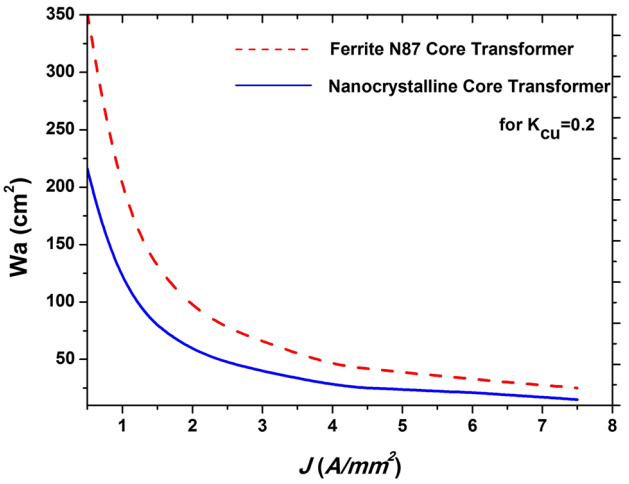


Fig. 4. Winding region changes according to the current density.

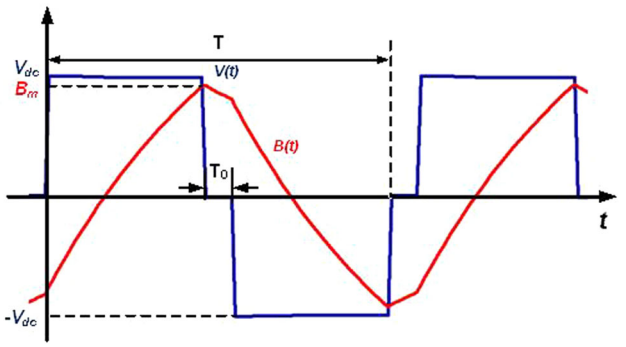


Fig. 6. Variation of magnetic flux in the case of a rectangular wave excitation.[9,28]

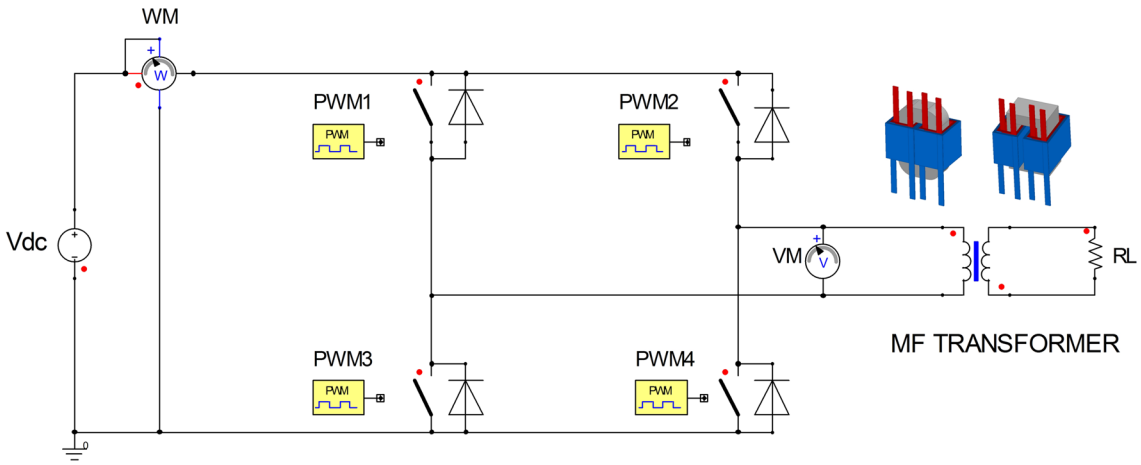


Fig. 5. Single-phase full-bridge inverter circuit.[4]

**Table V. Core loss coefficients of core materials**

| Core material type | $K_h$ | $K_c$ | $K_e$ |
|---|---|---|---|
| Ferrite N87 | 0.0032 | $2.43 \times 10^{-6}$ | $1.55 \times 10^{-5}$ |
| Nanocrystalline | 0.0021 | $1.91 \times 10^{-7}$ | $1.22 \times 10^{-6}$ |

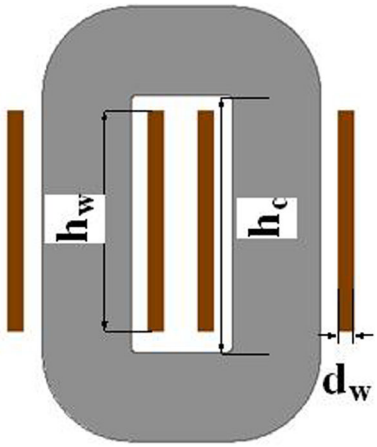


Fig. 7. Transformer winding parameters.

In this expression, the proximity effect varies with the square of the winding layer quantity ($m$). The skin and the proximity effects coefficients ($\xi_1$ and $\xi_2$) are given in Eqs. 11 and 12, respectively.[27,28,30]

$$\xi_1 = \frac{\sinh(2\Delta') + \sin(2\Delta')}{\cosh(2\Delta') - \cos(2\Delta')} \tag{11}$$

$$\xi_2 = \frac{\sinh(\Delta') - \sin(\Delta')}{\cosh(\Delta') + \cos(\Delta')} \tag{12}$$

As expressed in Eq. 13, the skin effect varies with the conductor material types. Furthermore, although the internal resistance of the aluminum foil is higher than the copper conductor, its skin thickness ($\delta$) is larger than the copper conductor for the same frequency value.[28]

$$\delta = \sqrt{\frac{2}{\omega\mu\sigma}} \text{ or } \delta = \sqrt{\frac{\rho}{\pi\mu f}} \tag{13}$$

The effect of the varying depth ratio ($\Delta$) depending on the frequency value is given in Eq. 14.

$$\Delta = \frac{d_w}{\delta} \tag{14}$$

As it is seen, the effect of varying ($\Delta$) depending on the frequency value is related to the equivalent conductor thickness. In this study, $\Delta$ is calculated as 0.4/0.85 for a 10-kHz operating frequency and 0.4 mm thickness of the aluminum foil ($d_w$). The porosity factor ($\eta_w$) of a solid winding is the ratio of window height ($h_c$) to foil winding height ($h_w$), as given in Eq. 15 and Fig. 7.[28]

$$\eta_w = \frac{h_w}{h_c} \tag{15}$$

In this study, $\eta_w$ is calculated as approximately 100/120 for the proposed transformer models. When the penetration depth ratio is rearranged with the porosity factor of the winding, Eq. 16 is obtained.[28] Thus, the rearranged depth effect ratio ($\Delta'$) can be calculated as approximately 0.43 for the transformer windings.

$$\Delta' = \sqrt{\eta_w}\Delta \tag{16}$$

Resistance values of the transformer's primary and secondary winding with C-core Nanocrystalline were obtained from the FEA model and are given in Table VI and Fig. 8. Because the secondary winding wounds around the primary winding, the volume and the resistance of the secondary winding become higher than the primary winding.

Since dimensions of the ferrite core transformer are bigger, its leakage flux values are normally different. This leads to a difference in the input impedances values of two designed transformers. This causes small differences between the input current values for the same operating frequency. In addition, this situation may have a slightly negative effect on voltage regulation. Inductance parameters of the nanocrystalline and the ferrite core transformers are shown in Table VI.

It can be seen that since the type of transformer core material affects the sizing of the transformer, it also affects the core losses and leads to differences in the resistance values of the windings. Therefore, the lower flux and the permeability values increase the transformer volume and affect the winding losses.

The AC resistance values of the primary and secondary windings are calculated depending on the operating frequency by the FEA parametric solver. The obtained results are given in Fig. 9a and b, respectively. It is seen from these figures that the AC resistance values of the ferrite core transformer windings are greater than the resistance values of the nanocrystalline core transformer windings. It can be said that the selected magnetic material affects the volume and AC resistance value of the windings and it consequently affects the losses, too.

In order to examine the current density of the windings dynamically, Fig. 10 compares the dispersion according to a maximum 400 A/cm$^2$ current density value. It has been determined that the AC resistance value of the transformer winding with

**Table VI. Equivalent circuit parameters of the transformer for a 10-kHz operating frequency**

| Design type | $L_{lk\text{-}p}$ (μH) | $L_{lk\text{-}s}$ (μH) | $L_M$ (mH) | $R_{fe}$ (kΩ) | $R_{ac\text{-}p}$ (kΩ) | $R_{ac\text{-}s}$ (kΩ) | $N1/N2$ | $U_{sc}$ (%) |
|---|---|---|---|---|---|---|---|---|
| Ferrite N87 core | 1.78 | 5.92 | 5.8 | 1.25 | 10.2 | 12.8 | 24/24 | 6.5 |
| Nanocrystalline core | 1.27 | 5.37 | 6.2 | 5.34 | 12.9 | 16.7 | 24/24 | 4.8 |

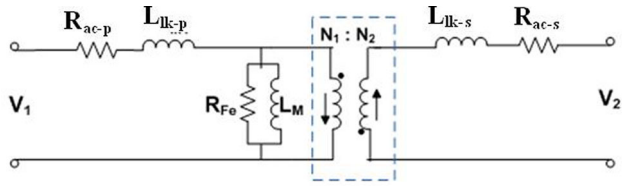


Fig. 8. Transformer equivalent circuit parameters according to the core structure.[5]

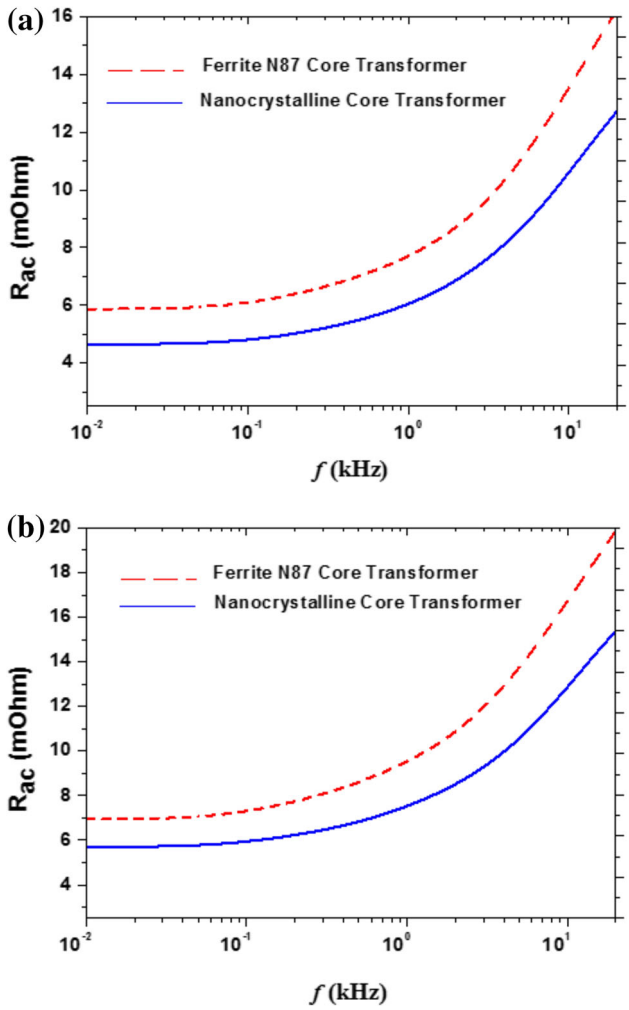


Fig. 9. AC resistance value according to the different core structure; (a) primary winding resistance, (b) secondary winding resistance.

ferrite N87 core material is higher and therefore, power dissipation and resultant temperature is higher at the upper and lower edges of the foil.

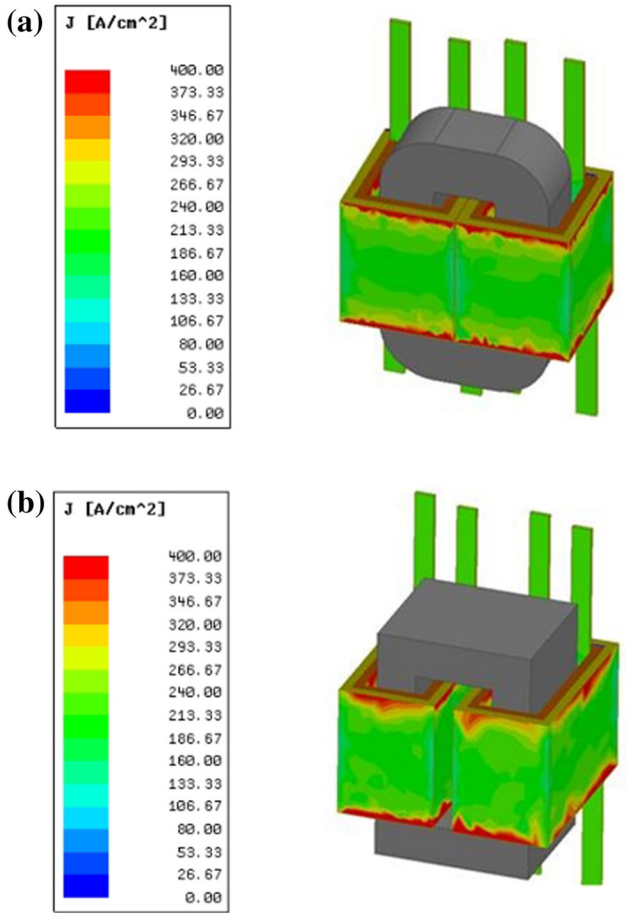


Fig. 10. Current density distributions; (a) the nanocrystalline core transformer, (b) the ferrite N87 core transformer.

**Table VII. Losses of the transformers**

| Design type | Core losses (W) | Winding losses (W) | Total losses (W) |
|---|---|---|---|
| Ferrite N87 core | 128 | 150 | 278 |
| Nanocrystalline core | 30 | 125 | 155 |

The current density on the surface of the foil is not homogeneously distributed due to the skin and the proximity effects caused by the frequency value. Reducing the number of layers of foil by wrapping or dividing the windings are the best two convenient methods in order to minimize these effects. The primary and the secondary windings of the modeled

**Table VIII. Mechanical properties of the transformers**

| Design type | Core volume ($cm^3$) | Core weight (kg) | Winding volume ($cm^3$) | Winding weight (kg) | Total weight (kg) |
|---|---|---|---|---|---|
| Ferrite N87 core | 1614 | 7.8 | 750 | 2.1 | 9.9 |
| Nanocrystalline core | 903.6 | 6.5 | 600 | 1.6 | 8.1 |

transformer have been divided into two identical parts. Thus, the increase of the AC resistance values of the windings has been maintained at an acceptable level.

## PERFORMANCE ANALYSIS WITH THE FEA

The MF transformers with the ferrite N87 and the nanocrystalline cores were modeled as shown in Fig. 11 using Maxwell 3D software in order to compare their performances. These two transformers were analyzed at the same operating frequency values, excitation waveform types, and power levels. Thus, the performance of both core materials can be distinguished clearly.

Transformer loss data under the rectangular waveform excitation is given in Table VII. As shown in the table, the core loss of the transformer with a nanocrystalline core is approximately four times less than the transformer with a ferrite core for the same power. Additionally, larger volume of the ferrite core leads to larger winding volume and thus higher winding losses, too.

As seen from the Table VII, the total loss of the nanocrystalline core transformer is lower than the ferrite core transformer. This means that the selection of the nanocrystalline core leads to a more effective transformer design. Besides, the ferrite core blocks limit the transformer power capacity. Therefore, the nanocrystalline core material seems more feasible for MF transformers, especially for high-power capacity.

Furthermore, mechanical performances of the designed transformers with different core materials are investigated and summarized in Table VIII. It is seen that both the core volume and the winding volume of the ferrite core transformer are higher than those of the nanocrystalline core transformer. Thus, a more compact structure can be obtained when the nanocrystalline core is used in the MF transformer design for the same power and operating frequency.

Flux distributions of the transformers obtained by the FEA are shown in Fig. 12. The ferrite core and the nanocrystalline core transformers at the 10-kHz operating frequency are dimensioned for max 0.3 T, respectively. It is seen that the maximum flux

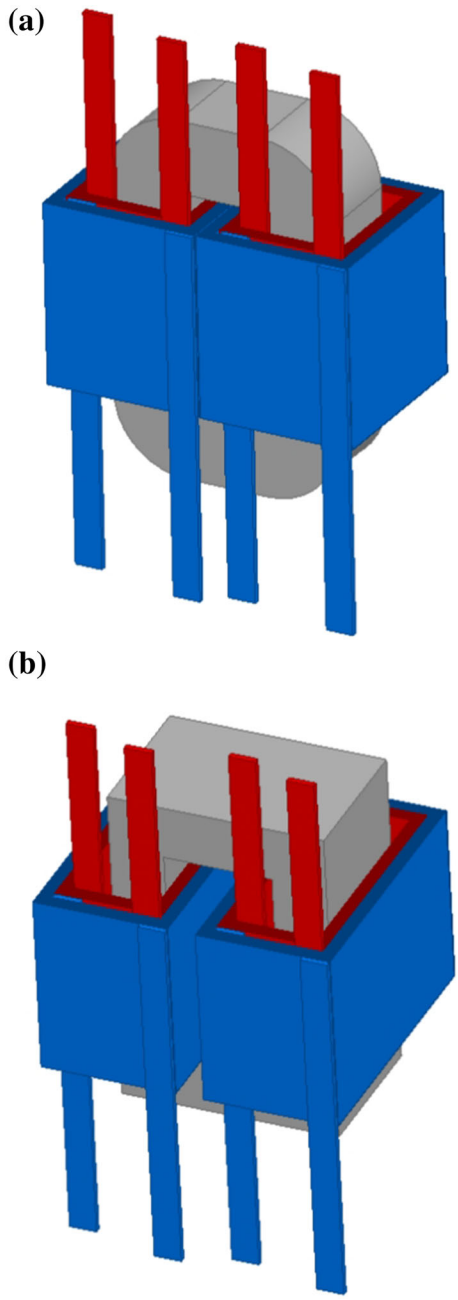


Fig. 11. MF transformers with the different core materials; (a) the nanocrystalline C-core, (b) the ferrite N87 block core.

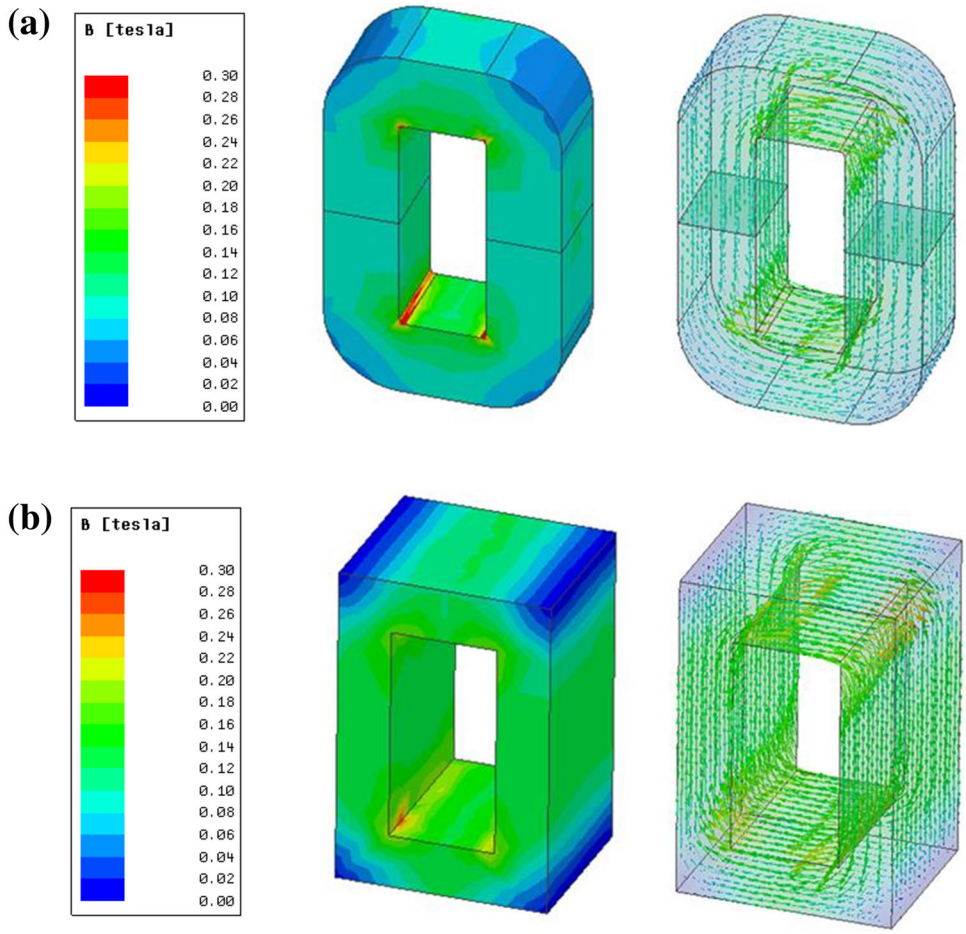


Fig. 12. Flux distributions; (a) the nanocrystalline C-core, (b) the ferrite N87 block core.

density, which is predefined for the design process for both material types, is not exceeded.

## CONCLUSION

In this study, two different MF transformers for a 35-kVA power and 10-kHz operating frequency were designed with a ferrite material core and a nanocrystalline material core to provide comparison between these materials. Effects of the core material on size, losses, and efficiency have been examined in detail. Differences on the saturation flux value and the specific core loss values affect the total size, the weight, and total losses of the transformer. Consequently, specifications of the core material used in the MF transformer affect both core and winding volumes and losses. The results prove that the MF transformer with the nanocrystalline core has better features in terms of size, volume, weight, and total losses. Core and winding losses of the nanocrystalline core transformer are approximately four times and 1.2 times less than the ferrite core transformer, respectively. Finally, total losses of the nanocrystalline core transformer are 1.8 times less than the ferrite core transformer. In addition, the core volume and weight of the transformer is reduced by 710 $cm^3$ and 2 kg, respectively, by using the nanocrystalline core. Similarly, total winding volume and weight are reduced by 150 $cm^3$ and 0.5 kg, respectively. This situation becomes more important at high power levels.

This means that the nanocrystalline core becomes more efficient and compact for the production of an MF transformer design. In addition, the nanocrystalline material is suitable to produce bigger cores that are limited to high power levels. Therefore, the nanocrystalline core material is quite convenient according to both the core and the winding dimension criteria for medium-frequency, medium- and high-power applications.

## REFERENCES

1. Villar, L. Mir, I. Etxeberria-Otadui, J. Colmenero, X. Agirre, and T. Nieva, *IEEE Energy Conversion Congr. and Exposition (ECCE)* (2012), pp. 684–690.
2. I. Sefa, N. Altin, S.Ozdemir, and M. Demirtas, *IEEE 19th Int. Symp. on Power Elect., Elec. Drives, Automation and Motion (SPEEDAM)* (2008), pp. 662–666.
3. I. Sefa, N. Altin, S. Ozdemir, and O. Kaplan, *IET Renew., Power Gen.* 9, 7 (2015).

4. N. Altin, S. Balci, S. Ozdemir, and I. Sefa, *IEEE Int. Conf. on Renewable Energy Research and Appl. (ICRERA)* (2013), pp. 1228–1233.
5. S. Balci, I Sefa, and M.B. Bayram, *IEEE-16th Int. Power Electron. and Motion Control Conf. and Expo. (PEMC)* (2014), pp. 861–866.
6. W.R. Wieserman, G.E. Schwarze, and J.M. Niedra, *NASA/TM-2005-213997, AIAA-2005-5720* (2005).
7. S. Balci, Gazi University, M.Sc. Thesis, 2010.
8. E. Agheb, H.K. Høidalen, and I.E.T. Electr, *Power Appl.* 7, 5 (2013).
9. T. Hatakeyama, K. Onda, and I.E.E.E. Trans, *Power Electron.* 29, 12 (2014).
10. D. Aguglia, and M. Neuhaus, *15th European Conf. on Power Electron. and Appl. (EPE)* (2013), pp. 1–8.
11. I. Sefa, S. Balci, and M.B. Bayram, *6th Int. Conf. on Electron. Computers and Artificial Intelligence (ECAI)* (2014), 43–48.
12. X. Liu, Y. Wang, M.R. Islam, G. Lei, C. Liu, and J. Zhu, *17th Int. Conf. on Electrical Machines and Systems (ICEMS)* (2014), pp. 2028–2032.
13. R. Garcia, A. Escobar-Mejia, K. George, and J.C. Balda, *5th Int. Symp. on Power Electron. for Distributed Gener. Syst. (PEDG)* (2014), pp. 1–6.
14. I. Villar, A. Rufer, U. Viscarret, and F. Zurkinden, *IEEE Int. Symp. on Ind. Electron. (ISIE)* (2008), pp. 208–213.
15. H.L. Chan, K.W.E. Cheng, T.K. Cheung, and C.K Cheung, *2nd Int. Conf. on Power Electron. Syst. and Appl. (ICPESA)* (2006), pp. 165–169.
16. J. Friebe and P. Zacharias, *IEEE Trans. Magn.* 50, 3 (2014).
17. W. Shen, F. Wang, D. Boroyevich, and C.W. Tipton, *IEEE Trans. Power Electron.* 23, 1 (2008).
18. Z.M. Shafik, K.H. Ahmed, S.J. Finney, and B.W. *5th IET Int. Conf. on Power Electron., Machines and Drives (PEMD)* (2010), pp 1–6.
19. K. Soltanzadeh, A. Tavakoli, and P.B. Arbab, *17th Conf. on Elect. Power Distribution. Netw. (EPDC)* (2012), pp. 1–8.
20. F. Sixdenier, J. Morand, O.A. Salvado, and D. Bergogne, *IEEE Trans. Magn.* 50, 4 (2014).
21. L.K. Varga, *J. Electron. Mater.* 43, 1 (2014).
22. M.S. Rylko, K.J. Hartnett, J.G. Hayes, and M.G. Egan, *24th Annu. IEEE Applied Power Electron. Conf. and Expo. (APEC)* (2009), pp. 2043–2049.
23. J.N. Calata, G.-Q. Lu, and K. Ngo, *J. Electron. Mater.* 43, 1 (2014).
24. Vitroperm 250F nanocrystalline core material, Vacuumschmelze, http://www.vacuumschmelze.de/. Accessed 15 November 2015.
25. FT-3 M nanocrystalline core material, http://www.hilltech.com/pdf/hl-fm10-cFinemetIntro.pdf, Accessed 10 November 2015.
26. TDK Ferrites and accessories, FERRIT material N87, http://en.tdk.eu/blob/528882/download/4/pdf-n87.pdf, Accessed 15 November 2016.
27. C.W.T. McLyman, *Transformer and Inductor Design Handbook*, 3rd ed. (Marcel Dekker, Inc., 2004), pp. 5.1–5.21.
28. I. Villar, EPFL Lausanne, Dissertation THÈSE NO 4622, 2010.
29. H. Gor and E. Kurt, *Int. J. Hydrogen Energ.* (2016). doi: 10.1016/j.ijhydene.2015.12.172.
30. P. Dowell, *Proc. IEEE* 113, 8 (1966).